PHYSICAL REVIEW B VOLUME 49, NUMBER 7 15 FEBRUARY 1994-I

Two-dimensional ^{13}C NMR study of orientational ordering in solid C_{60}

R. Blinc, J. Seliger, J. Dolinšek, and D. Arčon
J. Stefan Institute, University of Ljubljana, 61111 Ljubljana, Slovenia

(Received 19 April 1993; revised manuscript received 15 October 1993)

Two-dimensional "separation of interactions" ^{13}C NMR spectra of powdered C_{60} have been measured between 13.8 and 280 K and the results are compared with various theoretical models. The data show that above $T_c=260$ K the C_{60} molecules reorient nearly isotropically and that at least two different motional processes are involved below T_c: A relatively slow process corresponding to the flipping of the axis of rotation and a fast one corresponding to uniaxial rotation of the C_{60} molecules around this axis. The spectra below T_c are compatible with a pseudorandom sequence of small amplitude uniaxial reorientations around at least three different axes separated by 60° leading to the same two nearly degenerate states as originally suggested. The spectra definitely rule out any uniaxial reorientations around a single axis. A linewidth transition was observed around 150 K in the homogeneous line shape reflecting the freezing in of the flipping of the rotational axis. Below 90 K also the uniaxial rotation slowly freezes out and the spectra gradually change into a static powder pattern as $T\rightarrow 0$.

I. INTRODUCTION

The high-temperature phase I of solid C_{60} represents a nearly ideal "plastic" solid with dynamic orientational disorder of the C_{60} molecules which form a face-centered-cubic lattice[1] with four molecules per cubic cell and a space group $Fm\bar{3}m$. All carbon sites in the C_{60} molecule are chemically equivalent. The individual C_{60} molecules are—according to coherent[2] quasielastic neutron-scattering measurements—undergoing[1,2] uncorrelated isotropic random reorientations through a continuum of orientations resulting in a time averaging of the truncated icosahedron to spherical symmetry.[2] NMR studies,[3,4] are consistent with this interpretation and show that the molecular reorientation time is at 283 K only three times longer ($\tau=9.1\times10^{-12}$ s) than the one expected for free rotation.[4] Around $T_{c1}=260$ K, solid C_{60} undergoes a structural phase transition of first order and the reorientational correlation time decreases to 2×10^{-9} s.[3,4] The transition occurs at the Brillouin-zone boundary. The space group is now $Pa\bar{3}$ with four orientationally nonequivalent molecules per unit cell and a simple cubic lattice.[1] According to neutron-scattering data,[1,2,5] long-range orientational order develops below T_{c1} and the molecules are librating around their equilibrium positions while undergoing occasional uniaxial jump reorientations between two nearly degenerate equilibrium states separated by 60°.[5] The reorientations take place about the $\bar{3}$-fold $\langle 111\rangle$ axis[5] so that six symmetry-related sites are involved. The two nearly degenerate orientations below T_{c1} should differ in energy by $\Delta E=11.4$ meV, and should be separated by an energy barrier of $E=290$ meV.[5] This two-state reorientation model has been successfully used to describe a large number of macroscopic properties of solid C_{60} at lower temperatures, e.g., the time-temperature dependence of the thermal conductivity[6] and of the thermal expansivity.[7]

High-resolution powder neutron-diffraction data[5] also show the existence of a cusp in the temperature dependence of the cubic-lattice constant at $T_{c2}=90$ K. The transition seems to be of second or higher order and seems to involve no change in crystal symmetry. Below T_{c2} in phase III, neutron-scattering data[5] show an orientationally ordered structure, although a small amount of static disorder still persists down to the lowest temperatures studied (5 K). This disorder amounts to 2 out of 12 nearest neighbors adopting the "wrong" configuration thus relieving the small degree of frustration involved with orientational ordering of icosahedral molecules in the $Pa\bar{3}$ structure.[5] These observations lead to an important question regarding the nature of the phase transition and the structure of solid C_{60}. Are the C_{60} molecules in phase I really undergoing uncorrelated fast isotropic rotations? Are the molecules in phase II indeed performing only jumps around the $\langle 111\rangle$ axis between two nearly degenerate states? Is the transition at 90 K a real structural phase transition in the thermodynamic sense or do we deal with a pure kinetic effect and/or a "glass" transition? Is the ground state of C_{60} orientationally ordered or do we deal with an orientational glass? Is the disorder in phase III completely static or is it dynamic and only appears to be static on the neutron-scattering time scale?

Recently David *et al.*[8] observed that purely uniaxial reorientations below T_{c1} would be inconsistent with the muon spin rotation (μSR) linewidth data[9] recorded for the labeled adduct Mu-C_{60}. They proposed an alternative model[8] involving a pseudorandom sequence of uniaxial reorientations leading to quasi-isotropic behavior below T_{c1}. It should be stressed that the above quasi-isotropic alternative model takes the C_{60} molecules between the very same two nearly degenerate orientations as the original two-state model. The difference is, however, that it involves a number of intermediate states.

One-dimensional (1D) and two-dimensional (2D) ^{13}C NMR line-shape data may help to answer some of the above questions. It is the purpose of this paper to throw some additional light on the microscopic nature of the molecular motion and the nature of the phase transitions in solid C_{60} via a comparison of 2D and 1D experimental and theoretical ^{13}C NMR line shapes. The theoretical powder line shapes were computed as a function of the C_{60} reorientational rate for (i) an isotropic rotational diffusion-type random walk of the C_{60} icosahedra yielding in the fast-motion limit the same NMR spectrum as free rotation, (ii) a uniaxial reorientation around the $\bar{3}$-fold $\langle 111 \rangle$ axis with jumps between two nearly degenerate equilibrium states involving six sites separated by 60°, (iii) a small amplitude uniaxial rotational diffusion-type random walk of the C_{60} icosahedra with a fixed axis of rotation, and (iv) a random sequence of successive uniaxial reorientations around three twofold axes $\langle 1\bar{1}0 \rangle$, $\langle 0\bar{1}1 \rangle$, and $\langle 101 \rangle$, separated by 60°. The random-walk steps amount here to 36° as suggested by David *et al.*[8]

II. EXPERIMENTAL RESULTS

The sample used was obtained from the Texas Fullerene Company. It was recrystallized and its purity (better than 98%) checked by mass spectroscopy. No residual ^{13}C toluene solvent lines were seen. The presence of a small amount of C_{70} molecules—leading to additional free volume— cannot however, be definitely excluded though the corresponding lines were not seen in ^{13}C NMR. Two-dimensional "separation of interactions" ^{13}C

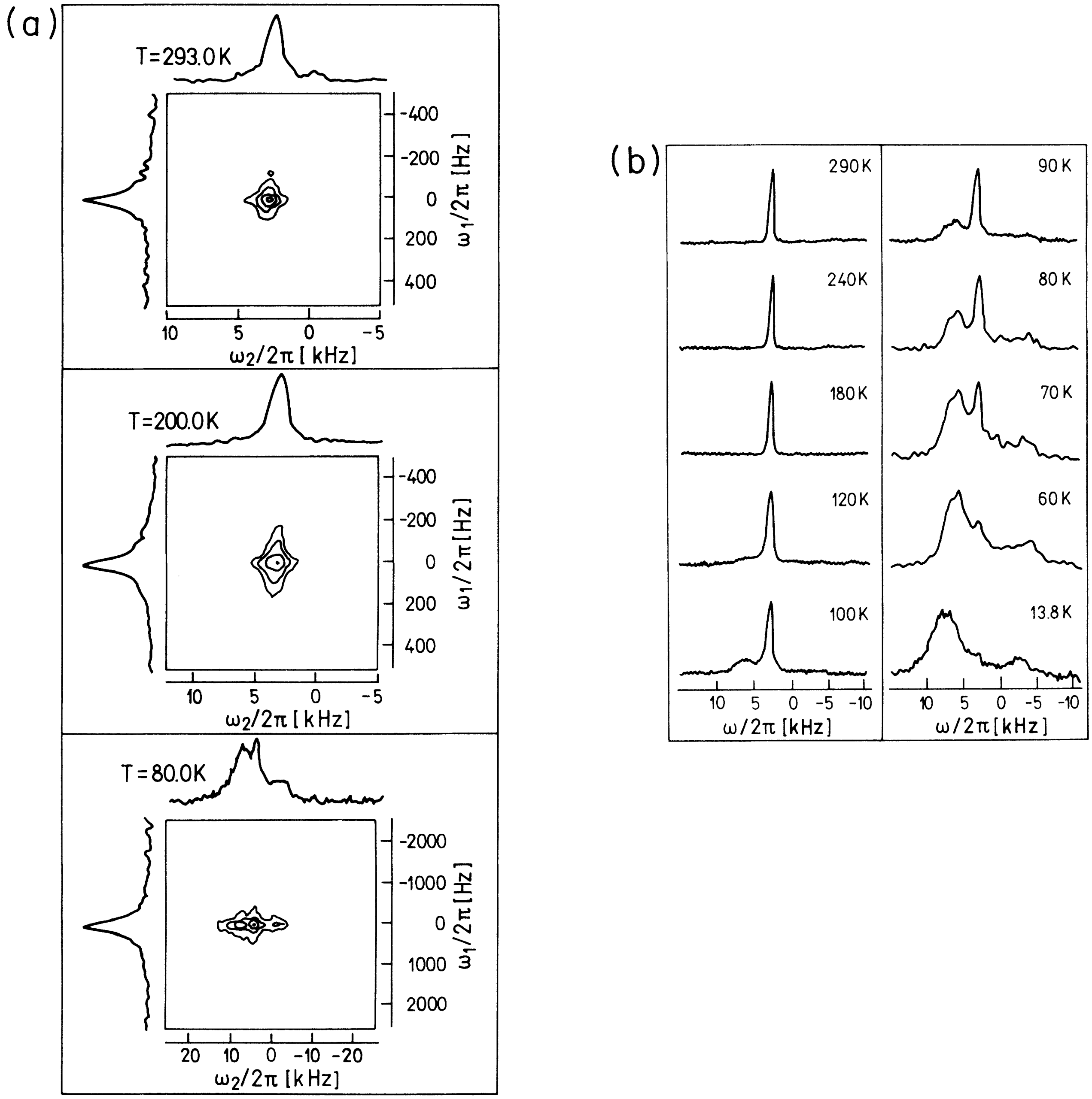

FIG. 1. (a) 2D ^{13}C NMR spectra of powdered C_{60} at various temperatures. (b) Projections on the ω_2 axis showing the 1D inhomogeneous ^{13}C NMR line shape in phases I, II, and III.

NMR spectra of powdered C_{60} have been measured at $\omega_L/2\pi = 67.925$ MHz with a temperature resolution of ± 0.05 K in the temperature range between 13.8 and 300 K. The pulse sequence was $90°\text{-}t_1/2\text{-}180°\text{-}t_1/2\text{-echo-}t_2$ plus phase cycling. The ω_1 domain yields the homogeneous line shape determined by ^{13}C dipole-dipole interactions while the ω_2 domain yields the inhomogeneous line shape determined by chemical shift and dipole-dipole interactions. The obtained 2D line shapes are shown in Fig. 1(a). The inhomogeneous linewidth reaches 20 kHz at low temperatures, whereas the homogeneous linewidth is here of the order of 200 Hz. At higher temperatures the homogeneous linewidth decreases to less than 50 Hz. The projections on the ω_2 axis [Fig. 1(b)] generally agree with the 1D spectra already published.[3,4] On the basis of the observed ^{13}C NMR line shapes, three different temperature regions can be distinguished.

(a) The range $T > 245$ K where we find a motionally narrowed NMR line of Lorentzian shape shifted by 4 kHz from the irradiation frequency 67.925 MHz. The shift corresponds to the isotropic part—145 ppm with respect to tetramethylsilane (TMS)—of the ^{13}C chemical-shift tensor.

(b) The range $90 < T < 245$ K where the inhomogeneous line shape gradually broadens and where around 160–170 K a linewidth transition was found in the homogeneous line shape. Below 120 K a broad shoulder in the inhomogeneous line shapes, shifted by 7.5 kHz from the irradiation frequency, appears in addition to the above narrow line centered at 4 kHz. This shoulder obviously corresponds to the singularity at $\sigma_\perp$ in the powder spectrum.

(c) The range $T < 90$ where the inhomogeneous line shape slowly changes into a static powder pattern. The most prominent feature in this range is the gradual exchange of intensities between the narrow line at 4 kHz and the broad shoulder at 7.5 kHz. This is best seen in the range between 90 and 60 K. Below 60 K the step discontinuity of the powder spectrum at $\sigma_\parallel$ is seen at -3 kHz.

No changes in the ^{13}C spectra were observed on going through $T_c = 260$ K.

The temperature dependence of the homogeneous ^{13}C line shapes is shown in Fig. 2. A linewidth transition centered at 150 K is clearly observed (Fig. 3). The homogeneous linewidth changes from 37 Hz above 200 K to ≈ 200 Hz below 150 K and does not show any further changes down to 80 K. The inhomogeneous line shape, on the other hand, still changes down to 50 K. This suggests that the observed homogeneous linewidth of 200 Hz does not correspond to the rigid lattice value. Obviously two different types of motion are involved: a slow motional process, which freezes out below 150 K, and a relatively fast process, which freezes out below 50 K. The first slow process has a correlation time of about

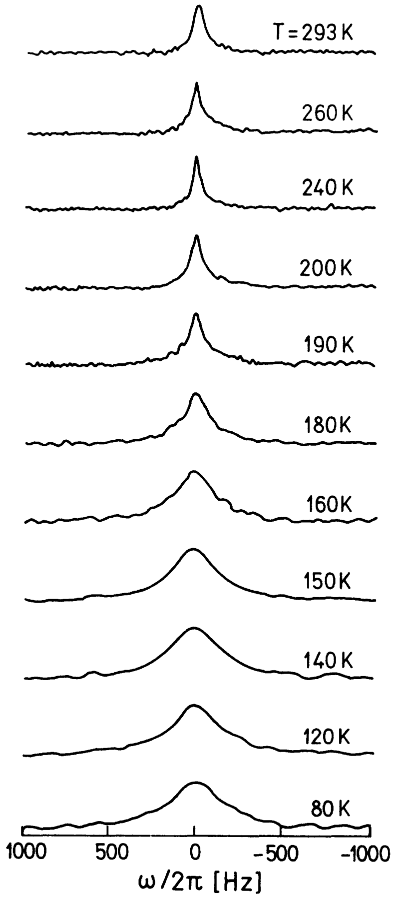

FIG. 2. Temperature dependence of the homogeneous ^{13}C NMR line shapes in powdered C_{60}.

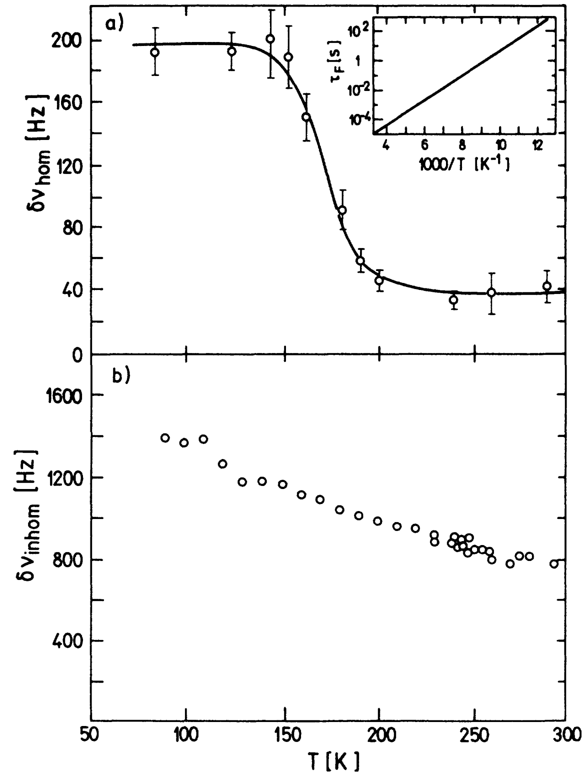

FIG. 3. Temperature dependence of the (a) homogeneous and (b) inhomogeneous linewidth of powdered C_{60}. The correlation time τ_F describing the flipping of the rotational axis is shown in the inset to 3(a). The width of the inhomogeneous spectra is determined at half height.

$\tau_F = 1$ ms at 160 K, whereas the second has a value $\tau_R \approx 14\ \mu$s at 60 K.

From a comparison of observed and calculated static-powder line shapes at 50 K, the components of the ^{13}C chemical-shift tensor relative to tetramethylsilane were determined as $\sigma_{xx} = 193$ ppm, $\sigma_{yy} = 182$ ppm, and $\sigma_{zz} = 40$ ppm. The axial asymmetry is significantly smaller than the one obtained at higher temperatures[4] where the molecular motion was not yet completely frozen out.

III. THEORY

The Hamiltonian of our problem is a sum of a Zeeman term, a chemical-shift term, and a dipole-dipole coupling term:

$$\mathcal{H} = \mathcal{H}_z + \mathcal{H}_{\text{cs}} + \mathcal{H}_{d\text{-}d} \ . \tag{1a}$$

The ^{13}C chemical-shift interactions

$$\mathcal{H}_{\text{cs}} = -\gamma \mathbf{B} \overleftrightarrow{\sigma} \mathbf{I} \tag{1b}$$

will determine the inhomogeneous NMR line shape of powdered C$_{60}$. Here $\overleftrightarrow{\sigma}$ is the ^{13}C chemical-shift tensor.

Since the natural abundance of ^{13}C is only 1.108%, ^{13}C dipole-dipole interactions are, over most of the temperature range, negligible as compared to the chemical-shift interactions, which amount to more than 10^4 Hz at the magnetic field used in this experiment. In a 2D "separation of interactions" experiment, on the other hand, the homogeneous linewidth, which is dominated by ^{13}C dipole-dipole interactions, can be determined separately.

Let us therefore first estimate the homogeneous part of the C$_{60}$ NMR linewidth which is due to the dipole-dipole coupling.

In the limit of fast isotropic C$_{60}$ reorientations, the intramolecular part of the ^{13}C dipole-dipole interactions[6] will be averaged out similarly as the ^{13}C chemical-shift tensor. What will remain is a part of the intermolecular dipolar interaction. The calculation proceeds as follows: The second moment of the dipolar line shape is given by the expression[10]

$$M_2 = \frac{3}{4}\left[\frac{\mu_0}{4\pi}\right]^2 \gamma^4 \hbar^4 I(I+1) \sum_k \overline{\left\langle \frac{(1-3\cos^2\Theta_{jk})}{r_{jk}^3} \right\rangle^2_{\text{motion}}} , \tag{2}$$

where the $\langle\ \rangle_{\text{motion}}$ indicates an average over the motion and the bar indicates the powder average. Here $\mu_0 = 4\pi \times 10^{-7}$ V m/As is the permeability of the vacuum, γ is the giromagnetic ratio of ^{13}C, r_{jk} is the distance between two dipoles, and Θ_{jk} is the angle between $\mathbf{r}_{jk}$ and the external magnetic field. The summation runs over all ^{13}C pairs on different C$_{60}$ molecules. Using

$$\mathbf{r}_1 = a(\sin\theta_1\cos\phi_1, \sin\theta_1\sin\phi_1, \cos\theta_1) \ , \tag{3a}$$

$$\mathbf{r}_2 = a(\sin\theta_2\cos\phi_2, \sin\theta_2\sin\phi_2, \cos\theta_2) \ , \tag{3b}$$

to specify the positions of the dipoles on the two spheres separated by $\mathbf{d} = (d,0,0)$ and

$$\begin{aligned}\mathbf{r}_{12} &= \mathbf{r}_1 - (\mathbf{d} + \mathbf{r}_2)\\ &= d(\epsilon(\sin\theta_1\cos\phi_1 - \sin\theta_2\cos\phi_2) - 1 \ , \epsilon(\sin\theta_1\sin\phi_1 - \sin\theta_2\sin\phi_2) \ , \epsilon(\cos\theta_1 - \cos\theta_2))\end{aligned} \tag{3c}$$

to specify the internuclear radius vector as well as

$$\mathbf{n}_B = (\sin\theta\cos\phi, \sin\theta\sin\phi, \cos\theta) \tag{3d}$$

to introduce the unit vector specifying the direction of the magnetic field, we obtain

$$\left\langle \frac{1-3\cos^2\Theta_{12}}{r_{jk}^3} \right\rangle_{\text{motion}} = \frac{1}{d^3} f(\epsilon,\theta,\phi) \ . \tag{3e}$$

Here $\cos\Theta_{12} = (\mathbf{r}_{12}\cdot\mathbf{n}_B)/|\mathbf{r}_{12}|$ and ϵ is the ratio between the radius of the C$_{60}$ sphere ($a = 3.54$ Å) and the distance d between the centers of the spheres. The correction parameter $f(\epsilon,\theta,\phi)$ is obtained numerically from the expression

$$f(\epsilon,\theta,\phi) = \left[\frac{1}{4\pi}\right]^2 \int_0^{\pi} \sin\theta_1 d\theta_1 \int_0^{\pi} \sin\theta_2 d\theta_2 \int_0^{2\pi} d\phi_1 \int_0^{2\pi} d\phi_2 F(\epsilon,\theta,\phi,\theta_1,\phi_1,\theta_2,\phi_2) \ , \tag{4a}$$

where $\theta_1, \theta_2, \phi_1, \phi_2$ are the polar and azimuthal angles describing the positions of the ^{13}C dipoles on the two spheres. Using

$$\begin{aligned} a^2 = {} & 1 + 2\epsilon^2[1 - \sin\theta_1\sin\theta_2\cos(\phi_1 - \phi_2)]\\ & -2\epsilon(\sin\theta_1\cos\phi_1 - \sin\theta_2\cos\phi_2) \end{aligned} \tag{4b}$$

and

$$\begin{aligned} b = {} & \epsilon[\sin\theta_1\sin\theta\cos(\phi - \phi_1) - \sin\theta_2\sin\theta\cos(\phi - \phi_2)\\ & + \cos\theta(\cos\theta_1 - \cos\theta_2)] - \sin\theta\cos\phi \end{aligned} \tag{4c}$$

one finds

$$F(\epsilon,\theta,\phi,\theta_1,\phi_1,\theta_2,\phi_2) = \frac{a^2 - 3b^2}{a^5} \ . \tag{4d}$$

After performing the powder average over $(1/d^6) f^2(\epsilon,\theta,\phi)$ and taking into account the natural abundance of the ^{13}C nuclei as appropriate for the case of the dipolar broadening in a magnetically diluted substance[10] and summing over first, second, and third nearest neighbors we find for the high-temperature fcc phase a dipolar half-width of the order of $\delta\nu = \sqrt{M_2}/2\pi = 42$ Hz. This is much less than in a static case where we—using the statistical theory of dipolar broadening in magnetically diluted substances[10]—find a Lorentzian line shape with a width at half height $\delta\nu = 334$ Hz.

The transition between these two limiting cases can be described by the well-known expression[10]

$$\delta\omega^2 = \delta\omega_0''^2 + \delta\omega_0'^2 \frac{2}{\pi} \tan^{-1}[\delta\omega\tau_c] \ . \tag{5}$$

Here $\delta\omega_0'^2$ is the part of the rigid lattice second moment that is destroyed by molecular motion, whereas $\delta\omega_0''^2$ is the part of the intermolecular interactions that is not averaged out as discussed above. $\delta\omega$ is the motionally narrowed homogeneous linewidth, and τ_c is the correlation time for the C_{60} reorientations.

Let us now turn to the inhomogeneous NMR line shape, which will be dominated by ^{13}C chemical-shift interactions.

The shape of the static NMR spectrum of a single crystal will depend on the orientations of the principal axes of the chemical-shift tensor with respect to the external magnetic field **B**. In case of molecular reorientations, the spectrum will, in addition, depend on the orientation of the chemical-shift tensor with respect to the reorientational axis.

We shall, for the sake of simplicity, assume that the ^{13}C chemical-shift tensors are axially symmetric with $\sigma_{\parallel} = \sigma_{zz} = 40$ ppm and $\sigma_{\perp} = \frac{1}{2}(\sigma_{xx} + \sigma_{yy}) = 187$ ppm. We also assume —unless stated otherwise—that the ^{13}C nuclei are distributed over a sphere with a constant probability, and that the rotational diffusion takes the system over a continuum of orientations.

Let us introduce a coordinate frame x,y,z where z is the rotational axis [Fig. 4(a)]. The direction of the external magnetic field **B** is in this frame described by the polar angle Θ_0 and the azimuthal angle Φ_0, so that we can define a unit vector

$$\mathbf{n}_B = [\sin\Theta_0\cos\Phi_0, \sin\Theta_0\sin\Phi_0, \cos\Theta_0] \tag{6}$$

pointing along the direction of **B**. The direction of the largest principal axis of the ^{13}C chemical-shift tensor is at $t = 0$ similarly described by the polar angle θ_0 and the azimuthal angle ϕ_0. At time t the corresponding angles are θ_0 and $\phi_0 + \phi(t)$. Thus we can introduce, in addition to $\mathbf{n}_B$, also a unit vector $\mathbf{n}(t)$ describing the instantaneous orientation of the ^{13}C chemical-shift tensor:

$$\mathbf{n}(t) = \{\sin\theta_0\cos[\phi_0 + \phi(t)], \sin\theta_0\sin[\phi_0 + \phi(t)], \cos\theta_0\} \ . \tag{7}$$

The instantaneous NMR frequency of the ^{13}C nucleus

$$\nu = \nu_L(1 - \sigma_{BB}) \tag{8}$$

is determined by the component σ_{BB} of the chemical-shift tensor along the direction of the external magnetic field

$$\begin{aligned}\sigma_{BB} &= \sigma_{\parallel}\cos^2\Theta(t) + \sigma_{\perp}\sin^2\Theta(t) \\ &= \sigma_{\perp} + (\sigma_{\parallel} - \sigma_{\perp})\cos^2\Theta(t) \ .\end{aligned} \tag{9}$$

Here $\Theta(t)$ is the angle between the instantaneous direction of the symmetry axis of the ^{13}C chemical-shift tensor and the magnetic-field direction

$$\begin{aligned}\cos\Theta(t) = \mathbf{n}(t)\cdot\mathbf{n}_B &= \sin\Theta_0\sin\theta_0\cos[\phi_0 + \phi(t) - \Phi_0] \\ &\quad + \cos\Theta_0\cos\theta_0 \ ,\end{aligned} \tag{10}$$

and ν_L the nucleus Larmor frequency.

The instantaneous NMR frequency can now be expressed as

$$\nu = \nu_0 + \Delta x \ , \quad 0 \le x \le 1 \ , \tag{11}$$

where

$$\begin{aligned} x &= \frac{\nu - \nu_0}{\Delta} = \cos^2\Theta(t) \ , \\ \nu_0 &= \nu_L(1 - \sigma_{\perp}) \ , \quad \Delta = \nu_L(\sigma_{\perp} - \sigma_{\parallel}) \ . \end{aligned} \tag{12}$$

Let us now first discuss a few limiting cases where the powder line shape can be determined analytically.

(a) In the static limit, we obtain for a powdered sample from the frequency distribution function $g(x)$

$$g(x) = \frac{1}{N}\frac{dN}{dx} = \frac{1}{N}\frac{dN}{d\Omega}\frac{d\Omega}{dx} = \frac{1}{2\sqrt{x}} \ , \quad 0 \le x \le 1 \tag{13}$$

the well-known square-root type expression for the NMR line shape. Here $\Theta \ne \Theta(t)$ and $d\Omega = 2\pi d(\cos\Theta)$ whereas

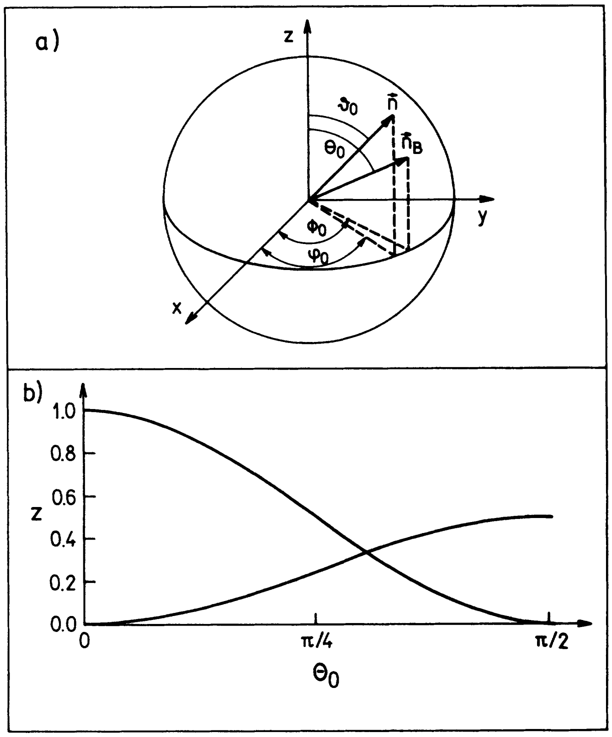

FIG. 4. (a) x,y,z coordinate frame showing the angles specifying the orientation of the rotational axis, the direction of the external magnetic field, and the direction of the largest principal axis of the ^{13}C chemical-shift tensor. (b) Upper and lower limits of the time-averaged NMR frequency z as a function of the polar angle Θ_0 for the case of the fast uniaxial rotation.

dN/dx is the number of the nuclei in the reduced frequency interval dx. The spectrum has a singularity at $\nu=\nu_L(1-\sigma_\perp)$ and a shoulder at $\nu=\nu_L(1-\sigma_\parallel)$.

(b) In the limit of the fast isotropic rotation, we have to average $x=\cos^2\Theta(t)$ over a sphere and find

$$z=\langle x\rangle=\tfrac{1}{3} \tag{14}$$

so that

$$\nu=\nu_0+\frac{\Delta}{3}=\nu_0(1-\tfrac{1}{3}\mathrm{Tr}\overleftrightarrow{\sigma}) . \tag{15}$$

The ^{13}C NMR spectrum is in this limit a δ function at $\langle x\rangle=\frac{1}{3}$, e.g., at the same frequency $\nu_0(1-\frac{1}{3}\mathrm{Tr}\overleftrightarrow{\sigma})$ as in a liquid solution of C_{60}.

(c) In the limit of fast uniaxial rotation in a powdered sample where the rotational axis is randomly oriented with respect to the external magnetic field, the procedure is a little bit more involved.

First we have to average the NMR frequency over the uniaxial rotation at fixed Θ_0. We get

$$z=\langle x\rangle_{\phi(t)}=\tfrac{1}{2}\sin^2\Theta_0\sin^2\theta_0+\cos^2\Theta_0\cos^2\theta_0 \tag{16}$$

as

$$\langle\cos[\phi_0+\phi(t)-\Phi_0]\rangle_{\phi(t)}=0 \tag{17a}$$

and

$$\langle\cos^2[\phi_0+\phi(t)-\Phi_0]\rangle_{\phi(t)}=\tfrac{1}{2} . \tag{17b}$$

It should be noted that—depending on the value of Θ_0—z varies between $\frac{1}{2}\sin^2\Theta_0$ and $\cos^2\Theta_0$. The upper and the lower limits of z as a function of Θ_0 are shown in Fig. 4(b).

The frequency distribution at fixed Θ_0 is now obtained from Eq. (16) and $d\Omega=2\pi d(\cos\theta_0)$ as

$$\begin{aligned} g_{\Theta_0}(z)&=\frac{1}{N}\frac{dN}{dz}=\frac{1}{N}\frac{dN}{d\Omega}\left|\frac{d\Omega}{dz}\right| \\ &=\frac{1}{4\cos\theta_0|\cos^2\Theta_0-\frac{1}{2}\sin^2\Theta_0|} . \end{aligned} \tag{18}$$

Using $u=\cos^2\Theta_0$ this can be written as

$$g_u(z)=\frac{\sqrt{2}}{\sqrt{(3u^2-1)(2z-1+u^2)}} . \tag{19}$$

Integrating over all possible orientations of the rotational axis with respect to $\mathbf{B}$, we find the motionally averaged inhomogeneous frequency spectrum for uniaxial rotation in a powdered sample as

$$g(z)=\frac{1}{2\sqrt{2}}\int_{\sqrt{z}}^{1}g_u(z)du , \quad 1\geq z\geq\tfrac{1}{2} , \tag{20a}$$

$$g(z)=\frac{1}{2\sqrt{2}}\left[\int_0^{\sqrt{1-2z}}g_u(z)du+\int_{\sqrt{z}}^{1}g_u(z)dz\right] , \quad \tfrac{1}{2}\geq z\geq\tfrac{1}{3} , \tag{20b}$$

$$g(z)=\frac{1}{2\sqrt{2}}\left[\int_0^{\sqrt{z}}g_u(z)du+\int_{\sqrt{1-2z}}^{1}g_u(z)dz\right] , \quad \tfrac{1}{3}\geq z\geq 0 . \tag{20c}$$

The spectrum exhibits a logarithmic singularity at $z=\frac{1}{3}$, e.g., at the position of the line for fast isotropic rotation. Its shape is shown in Fig. 5 together with the static spectrum and the spectrum for fast isotropic rotation. The residual linewidth in the fast-motion limit is here due to the fact that the component of the chemical-shift tensor parallel to the rotational axis is not averaged out by uniaxial rotation.

The transition from the fast- to the slow-motion limit has to be worked out numerically. The adiabatic NMR line shape is here obtained as a Fourier transform of

$$G(t)=\left\langle\left\langle\exp\left[i\int_0^t\omega(t')dt'\right]\right\rangle_{\text{motion}}\right\rangle_{\text{orientation}} , \tag{21}$$

where

$$\omega(t')=2\pi[\nu_0+\Delta\cos^2\Theta(t)] \tag{22a}$$

and $\cos\Theta(t')$ is given by expression (10). The line will be motionally narrowed whenever the motion is of sufficiently high symmetry and sufficiently fast so that the autocorrelation time τ for this motion satisfies the condition

$$\alpha=(\sigma_\parallel-\sigma_\perp)\gamma B_0\tau\ll 1 . \tag{22b}$$

Let us now look into the case of the gradual slowing down of stochastical ±60° jumps[5] of the C_{60} groups between two equilibrium states about the ⟨111⟩ direction, i.e., a motion involving three pairs of symmetry-related orientations. It is this type of motion which—according

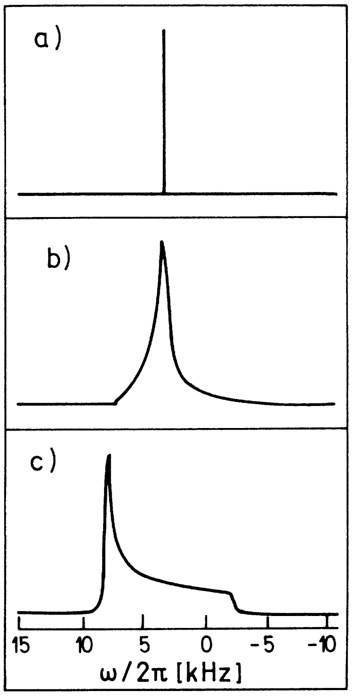

FIG. 5. Simulated inhomogeneous ^{13}C NMR line shape of powdered C_{60} for (a) fast isotropic reorientation, (b) fast uniaxial rotation, and (c) a static powder spectrum. In all three cases, the ^{13}C chemical-shift tensor was assumed to be axially symmetric.

to neutron-diffraction data[5]—dominates in phase II and freezes out ongoing to phase III at $T_{c2}=90$ K.

The computational procedure we used was as follows. Neutron-scattering data[5] indicate the existence of two nonequivalent free-energy minima for the rotation of the C_{60} groups around the $\langle 111 \rangle$ axis at $\Phi_1=98°$ and $\Phi_2=38°$. Because $\langle 111 \rangle$ is a $\bar{3}$-fold rotation axis, we have three sites corresponding to the orientation 1 at $\Phi_1=98°+k120°$, $k=0,1,2$, and three sites corresponding to the orientation 2 at $\Phi_2=38°+k120°$, $k=0,1,2$. The occupational probability for orientation 1 is "a" and for orientation 2 is "b" where

$$a+b=1 \ . \tag{23}$$

In order to make the problem tractable for a numerical procedure, we replaced the integral in expression (21) by a sum

$$\int_0^t \omega(t')dt'=T \sum_{m=t'/T=0}^{t/T} \omega_m(\theta_0,\Theta_0,\Psi_0=\phi_0-\Phi_0,\phi) \ , \tag{24}$$

where T is the dwell time.

We assumed that

$$\phi(n\tau)=\phi((n-1)\tau)\pm 60° \tag{25a}$$

resulting in a change $\omega_{\phi((n-1)\tau)} \rightarrow \omega_{\phi(n\tau)}$ whenever $t'=mT>n\tau$.

We further assumed that the probability to find a ^{13}C isotope in a C_{60} molecule is uniformly distributed over a sphere so that

$$\cos\theta_0=\text{random}([-1,1]) \ , \tag{25b}$$

that we deal with a powder sample resulting in

$$\cos\Theta_0=\text{random}([-1,1]) \ , \tag{25c}$$

and that

$$\phi_0-\Phi_0=\Psi_0=\text{random}([0,2\pi]) \ . \tag{25d}$$

The homogeneous rigid lattice linewidth was taken as $1/T_2=300$ Hz.

The adiabatic NMR line shape was now obtained from expression (21) by assuming a random walk between the two states involving six sites separated by 60° with the molecule spending the time $a\tau$ in state 1 and $b\tau$ in state 2. The temperature variation of a and b was taken from Ref. 5.

The resulting spectra are shown in Fig. 6 for different values of the correlation time τ and for the different occupational probabilities. For $\alpha=\nu_0(\sigma_\parallel-\sigma_\perp)\tau \gg 1$, we get a typical powder pattern appropriate for an axially symmetric chemical-shift tensor. With decreasing α, the spectrum slowly changes and a new shoulder starts to appear at the right-hand side of the $\nu=\nu_L(1-\sigma_\perp)$ singularity. The shoulder changes into a pronounced second peak, and for $\alpha=0.4$, the shoulder is already much stronger than the former singularity. Below $\alpha=-0.1$ it is the only peak which remains in the spectrum. A small deviation of the occupational probabilities from $a=b=0.5$ has no significant influence on the line shape.

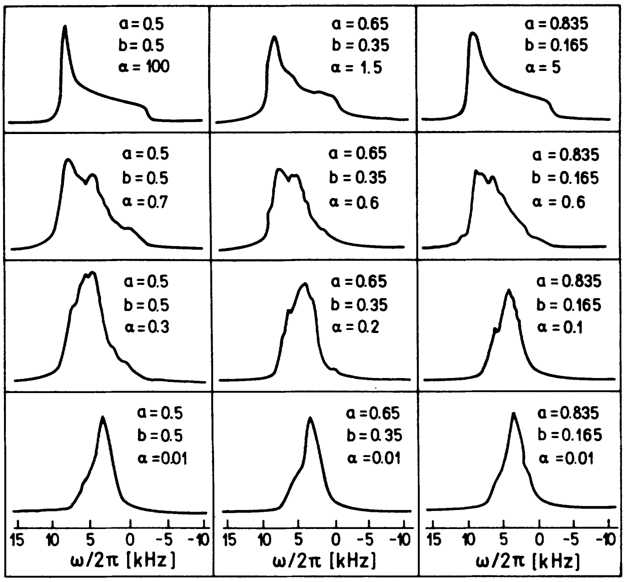

FIG. 6. Simulated ^{13}C NMR line shapes of powdered C_{60} for the case of uniaxial random jumps around the $\bar{3}$-fold $\langle 111 \rangle$ axis between three pairs of nearly equivalent equilibrium orientations separated by 60°, i.e., the two-state model (Ref. 5). The spectra are evaluated for different normalized reorientational rates $\alpha=(\sigma_\parallel-\sigma_\perp)\gamma B\tau$ and for different occupational probabilities for the orientation 1 "a" and for the orientation 2 "b."

The spectral shape approaches here the one obtained analytically for uniaxial rotation in the fast-motion limit. Even for $\alpha=0.01$, the line is still asymmetrically broadened with a half-width of about 5 kHz and far from the near δ function-type line shape found experimentally in phase II above 110 K.

The above calculation for the rotation about the $\langle 111 \rangle$ axis has been repeated for a discrete distribution of the ^{13}C sites. The C_{60} molecule was first approximated by an icosahedron with possible ^{13}C sites being given by the 12 icosahedral vertices. A random-walk-type exchange between neighboring sites appropriate for uniaxial rotation was assumed. The resulting spectra are—except for the residual shoulder at $\sigma_\perp$ arising from nuclei lying on the rotational axis—except for the residual shoulder at $\sigma_\perp$ arising from nuclei lying on the rotational axis— practically indistinguishable from the case where the possible ^{13}C sites were assumed to be homogeneously distributed over a sphere and the jumps were $\phi=\phi_0\pm 60°$. The same was found to be true for the case where the possible ^{13}C sites were assumed to be given by the 60 vertices of the ideal truncated icosahedron with 12 pentagonal and 20 hexagonal faces.[11] Here, however, the residual $\sigma_\perp$ shoulder disappears in the fast-motion limit.

Using the icosahedral approximation for the C_{60} molecule we also computed the ^{13}C NMR line shape as a function of the correlation time τ for the case of isotropic reorientation. Here we described the motion by a random walk among all the possible neighboring ^{13}C sites, e.g., neighboring icosahedral vertices.[11] Whereas for the case of uniaxial icosahedral rotation, the number of neighboring sites which can be reached in the random walk is two (except for the vertices on the rotational axis), the number of neighboring sites, available for random-walk-type jumps, is five here. The resulting spectra are shown in Fig. 7. In the fast-motion limit, we now obtain a narrow symmetric line of nearly Lorentzian shape. The shape is close to the one found experimentally in phase I above $T_{c1}=260$ K. It is also similar to the one found in the high-temperature part of phase II above 140 K. The transition from the fast- to the slow-motion limit results here in a different temperature dependence of the motionally narrowed line shapes than in the case of uniaxial rotation. None of the above-mentioned cases is, however, capable of describing the temperature dependence of the observed ^{13}C spectra in phases II and III.

To describe the temperature dependence of the spectra in phases II and III, we obviously have to introduce a more complicated model where the axis of uniaxial rotation occasionally flips. Following David *et al.*[8] we evaluated the powder line shape for a random sequence of successive uniaxial reorientations around three axes $\langle 1\bar{1}0\rangle$, $\langle 0\bar{1}1\rangle$, and $\langle 101\rangle$ separated by 60° (Fig. 8). We also assumed that the random-walk steps amount here to 36°.[8]

The correlation time τ_F for the flips of the rotational axis was assumed to be $\tau_F=K\tau_R$, where τ_R is a correlation time for the uniaxial reorientation. The spectra in Fig 9(a) have been computed for various K values and various τ_R and show a much better agreement with the experimentally observed spectra [Fig. 9(b)] than the pure uniaxial reorientation models. The temperature variation of $\alpha_R=\gamma B(\sigma_\parallel-\sigma_\perp)\tau_R$ and $\tau_F=k\tau_R$ has been determined by a comparison of the theoretical and experimental spectra (Fig. 9) and is shown in Fig. 10.

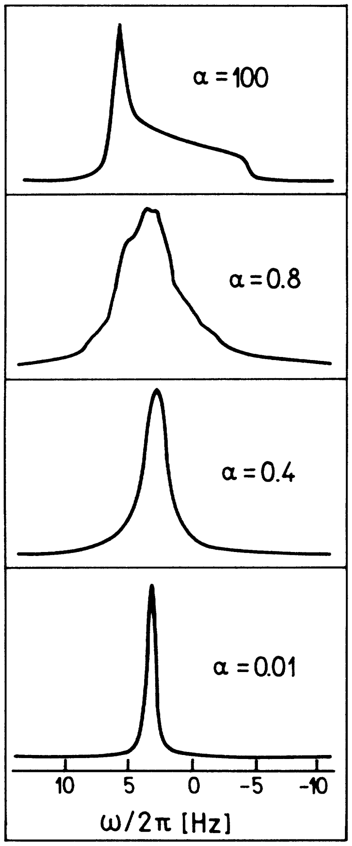

FIG. 7. Simulated inhomogeneous ^{13}C line shapes of powdered C_{60} for an isotropic random-walk-type rotational diffusion and different reorientation rates.

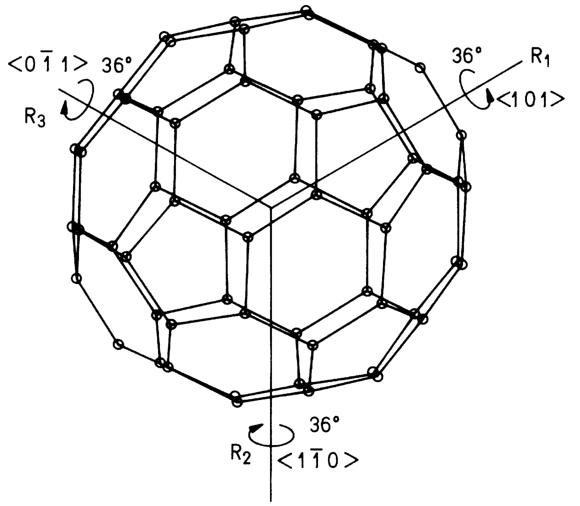

FIG. 8. Reorientational model involving a random sequence of successive uniaxial reorientations R_1, R_2, and R_3 around the $\langle 101\rangle$, $\langle 0\bar{1}1\rangle$, and $\langle 1\bar{1}0\rangle$ axes. Here $R_1=R_x(36°)R_y(-45°)$, $R_2=R_z(36°)R_x(-45°)$, and $R_3=R_x(36°)R_z(-45°)$. The probability for each of these rotations is the same.

It should be noted that a number of models, which involve other combinations of a flipping of the rotational axis, could yield similar spectra and that powder NMR by itself cannot uniquely determine what is really going on. It can, however, determine what is not going on, e.g., it can exclude certain models which are incompatible with the experiments, such as the two-state jump model for phase II.

IV. DISCUSSION AND CONCLUSIONS

A comparison between the observed and computed inhomogeneous ^{13}C spectra shows that the C_{60} molecules indeed reorient nearly isotropically and fast in phase I above T_{c1}.

There is no significant change in the line shape at T_{c1}. Though the reorientational correlation time increases by three orders of magnitude on cooling below T_{c1}, we are still in the fast-motion limit as far as the ^{13}C NMR line shape is concerned. The appearance of a $2^6=64$-pole order parameter[12]

$$\eta^{(m)}(l)=C_0\left\langle \sum_{i\in l} Y_6^m(\Theta_i,\Phi_i)\right\rangle\neq 0\ , \quad T<T_{c1} \tag{26}$$

in the orientational probability distribution function of the lth C_{60} molecule should indeed not produce any change in the NMR spectra. Here the $Y_6^m(\Theta_i,\Phi_i)$ are spherical harmonics of sixth order and the sum is over all

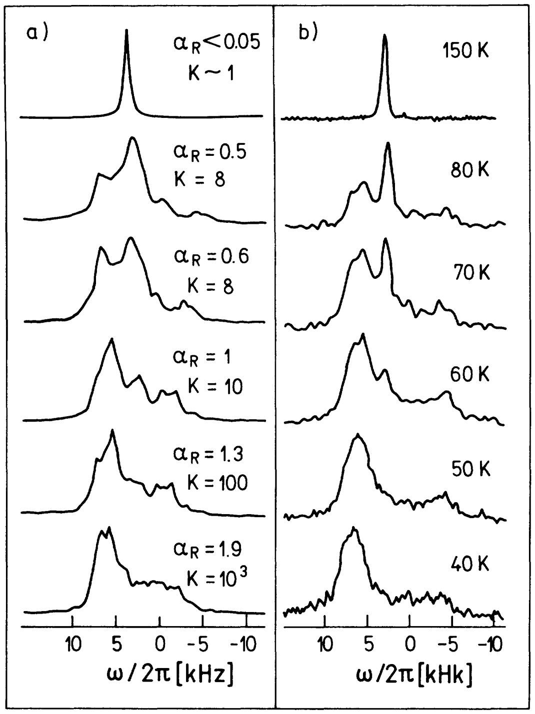

FIG. 9. (a) Simulated inhomogeneous ^{13}C NMR line shapes for a random sequence of successive 36°-step reorientations around three different rotational axes ⟨101⟩, $0\bar{1}1$⟩, and ⟨$1\bar{1}0$⟩ (Ref. 8) separated by 60°. The simulations were performed for different reorientation rates α and different K values covering the transition from the fast- to the slow-motion limit using a Debye model and $\tau_F = K\tau_R$. (b) Experimental ^{13}C spectra at various temperatures to be compared with simulated ones.

i atoms of a given C_{60} molecule.

The temperature dependence of the homogeneous ^{13}C NMR linewidth shows the occurrence of a NMR linewidth transition in phase II. In the high-temperature part of this phase, between 240 and 200 K, the residual linewidth is close to the one expected for nearly free rotation as suggested by neutron-scattering data[5] for phase I.

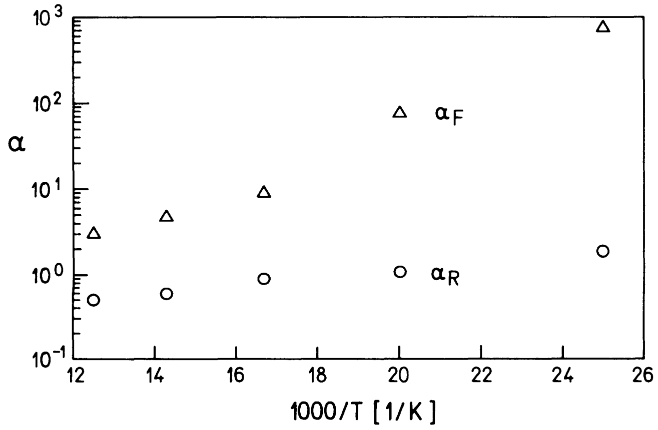

FIG. 10. Temperature dependence of $\alpha_R = \gamma B(\sigma_\parallel - \sigma_\perp)\tau_R$ and $\alpha_F = \gamma B(\sigma_\parallel - \sigma_\perp)\tau_F$.

In the low-temperature part of the phase II, below 120 K, the homogeneous linewidth (200 Hz) is lower than the value 334 Hz expected for a static cubic lattice of rigid C_{60} molecules. Thus, another linewidth transition should occur at still lower temperatures. The fact that this inhomogeneous line shape is on a time scale of 10 kHz still somewhat motionally averaged at 150 K suggests that (a) two different types of motion—a slow and a fast one—are involved, and (b) that the second linewidth transition where the fast motion would freeze out should occur at very low temperatures outside the temperature range where the homogeneous linewidth was studied (i.e., below 80 K). We believe that the slow motion, which has a value of $\tau_F \approx 1$ ms at 160 K, corresponds to the flipping of the rotational axis, whereas the fast motion, which is of the order of $\tau_R \approx 14$ μs at 60 K, corresponds to uniaxial rotation of C_{60}. It is this faster process which determines the T_1 spin-lattice relaxation data of Tycko *et al.*[3] and Johnson *et al.*[4] below the transition temperature T_{c1}. The combination of our inhomogeneous linewidth motional averaging data and the T_1 minima at 240 K in a 9.39-T field and at 233 K in a 7.04-T field seen by Tycko *et al.*[3] and Yannoni *et al.*[14] allows an estimate of the uniaxial rotational correlation time $\tau_R = \tau_{0,R}\exp(E_{a,R}/kT)$ with $\tau_{0,R} = 7\times10^{-11}$ s and $E_{a,R} = 64$ meV. The homogeneous linewidth transition data yield in the single correlation time approximation for the flipping of the rotational axis the correlation time $\tau_F = \tau_{0,F}\exp(E_a/kT)$, where $\tau_{0,F} = 2\times10^{-10}$ s and $E_a = 250$ meV [Fig. 3(a)]. The above values are, however, only order-of-magnitude estimates. Our data cannot exclude the existence of a distribution of correlation times.

The NMR data completely disagree with the interpretation of the early neutron-scattering results[5] as far as the reorientational motion in phases II and III is concerned. The C_{60} motion in phase II cannot be described as a simple uniaxial reorientation around ⟨111⟩ between two equilibrium states involving six symmetry-related orientations separated by 60°. The NMR spectra clearly show the following.

(i) The reorientational motion in phase II is not uniaxial but involves a flipping of the rotational axis and uniaxial rotations around this axis. The probability for the flipping of the axis of rotation becomes smaller as T_{c2} is approached from above. The spectra are compatible with a pseudorandom sequence of small amplitude uniaxial reorientations around three different axes[8] separated by 60° resulting in a quasi-isotropic reorientational motion, which gradually freezes out at lower temperatures. It should be stressed that the above quasi-isotropic alternative model takes the C_{60} molecules between the very same two nearly degenerate orientations as the original two-state model. The difference is, however, that it involves a number of intermediate states with lifetimes which are comparable to the residence times of the molecules in the two nearly degenerate orientations. If the lifetimes of these intermediate states would be significantly shorter than the residence times in the two degenerate orientations, the result for the NMR line shape would be the same as if we would have 60° uniaxial jumps between the two degenerate orientations in contrast to the experimental data. The data thus clearly show that below T_{c1} we do not have a two-state reorientational motion but a multistate multiaxes motion.

(ii) The orientational motion around a given axis involves small jumps between a large number of orientations. This agrees with recent suggestions[13] that below T_{c1} there exist many nearly degenerate orientations leading to glassy behavior with $T_{c2} \approx T_g = 90$ K.

The NMR spectra similarly show that phase III is not completely orientationally ordered and that a fair amount of fast uniaxial molecular reorientations takes place in this phase too. Below 70 K, this motion starts to become rather slow on the NMR time scale and $\gamma B(\sigma_{\parallel} - \sigma_{\perp})\tau$ becomes much larger than 1 as $T \rightarrow 0$. In view of the above facts we believe that the orientational ordering in solid C_{60} is much more complex than assumed so far.[13]

---

[1] P. A. Heiney, G. B. M. Vaughan, J. E. Fischer, N. Coustel, D. E. Cox, J. R. D. Copley, D. A. Neumann, W. A. Kamitakahara, K. M. Creegan, D. M. Cox, J. P. McCauley, and A. B. Smith, Phys. Rev. B **45**, 4544 (1992), and references therein.

[2] D. A. Neumann J. R. D. Copley, R. L. Cappalletti, W. A. Kamitakahara, R. M. Lindstrom, K. M. Creegan, D. M. Cox, W. J. Romanow, N. Coustel, J. P. McCauley, Jr., N. C. Maliszewskyj, J. E. Fischer, and A. B. Smith, Phys. Rev. Lett. **67**, 3808 (1991).

[3] R. Tycko, G. Dabbagh, R. M. Fleming, R. C. Haddon, A. V. Makhija, and S. M. Zahurak, Phys. Rev. Lett. **67**, 1886 (1991).

[4] R. D. Johnson, C. S. Yannoni, H. C. Dorn, J. R. Salem, and D. S. Bethune, Science **255**, 1235 (1992).

[5] W. I. F. David, R. M. Ibberson, T. J. S. Dennis, J. P. Hare, and K. Prassides, Europhys. Lett. **18**, 219 (1992), and references therein.

[6] R. C. Yu, N. Tea, M. B. Salamon, D. Lorents, and R. Malhotra, Phys. Rev. Lett. **68**, 2050 (1992).

[7] F. Gugenberger, R. Heid, C. Meingast, P. Adelmann, M. Braun, H. Wuhl, M. Haluska, and H. Kuzmany, Phys. Rev. Lett. **69**, 3774 (1992).

[8] W. I. F. David, R. M. Ibberson, T. J. S. Dennis, J. P. Hare, and K. Prassides, Europhys. Lett. **18**, 735 (1992).

[9] R. F. Kiefl, W. Schneider, A. MacFarlane, K. Chow, T. L. Duty, T. L. Estle, B. Hitti, R. L. Lichti, E. J. Ansaldo, C. Schwab, P. W. Percival, G. Wei, S. Wladek, K. Kojima, W. J. Romanow, J. P. McCauley, Jr., N. Coustel, J. E. Fischer, and A. B. Smith, Phys. Rev. Lett. **68**, 1347 (1992).

[10] A. Abragam, *The Principles of Nuclear Magnetism* (Clarendon, Oxford, 1961).

[11] A. B. Harris and R. Sachidanandam, Phys. Rev. B **46**, 4944 (1992).

[12] K. H. Michel, Chem. Phys. Lett. **193**, 478 (1992).

[13] J. P. Lu, X. P. Ling, and R. M. Martin, Phys. Rev. Lett. **68**, 1551 (1992).

[14] C. S. Yannoni, R. D. Johnson, G. Meijer, D. S. Bethune, and J. R. Salem, Am. Chem. Soc. **95**, 9 (1991).